Comprehensive Comparison Between Mechanical Properties of Nanofiber Matrix and Single Nanofibers

Fatemeh Jahanmard-Hosseinabadi and Mohammad Amani-Tehrani*

Abstract- **The development of electrospun nanofibers for using in different applications requires a comprehensive understanding of the mechanical properties of a single nanofiber and nanofiber layer. Here, we studied the mechanical properties of nanofiber layer and single nanofiber of polycaprolactone (PCL)/functionalized multiwall carbon nanotubes (F-MWCNTs) composite structures. Scanning electron microscopy (SEM) showed morphology and diameter of composite nanofibers with various CNT concentrations. Moreover, the tensile testing was used for measuring mechanical properties of both nanofiber layer and single nanofibers by distinct procedures. Our results clearly showed that the mechanical properties of single nanofibers had a significant difference with those of nanofiber layer. By increasing the F-MWCNT concentration up to 3 wt%, Young's modulus and tensile strength of the nanofiber layer increased. However, Young's modulus and tensile strength of single nanofiber increased with addition of F-MWCNTs up to 1 wt% and further increase in concentration led to a decrease in the modulus and tensile strength of single nanofiber.Moreover, the toughness and elongation-at-break of the nanofiber layer and single nanofiber showed different trends. Taken together, considering the mechanical properties of nanofibers in different scales, help us to design an appropriate structures for various applications.**

Keywords: **composite nanofibers, carbon nanotubes, mechanical property, single nanofibers, nanofiber layer**

I. INTRODUCTION

Electrospinning is a technique for producing micro/nanofiber layer from a rich variety of natural and synthetic polymers, as well as incorporating organic and inorganic nanomaterials in polymer fibers [1,2]. High surface-area-to-volume ratio of electrospun nanofibers made them as desired materials for a wide range of applications including tissue engineering [3,4], drug delivery [5,6], filtration [7,8], and biosensors [9,10].

For most of these applications, the mechanical properties of both nano- and macro-scale play an important role [11]. Moreover, tailoring mechanical property of electrospun nanofibers is an important step towards designing this structure for different applications [12].

However, the mechanical properties of nanofiber layer are largely predefined by the properties of the single nanofibers, other factors such as the interaction of nanofibers in the layer, fiber diameters, randomness structure can completely change the mechanical behavior of layer [12]. These differences show the critical need for mechanical characterization of nanofiber layer and single nanofibers.

Many strategies have been used to improve the mechanical properties of the electrospun nanofibers [13]. Incorporating inorganic materials is a method that increases mechanical properties of composite nanofibers. Carbon nanotubes (CNT) are one of the interesting materials due to their outstanding mechanical properties which are associated with their high aspect ratio [14].

The good dispersion of CNTs in a polymer layer can be important to fully utilize their exceptional properties [15,16]. The simultaneous functionalization of CNT and sonication may be helpful in achieving better CNT dispersion in polymer nanofibers. Therefore, the processing method of dispersing CNTs is one of the most important steps to obtain high-quality mechanical properties of nanofibers [17-19].

We proposed a new method for measuring the mechanical properties of PCL single nanofiber in our previous work [20]. In our recent work, the mentioned method was used for measuring the mechanical properties of single nanofiber of PCL with different percentage of CNTs. The novelty of this work is focused on the different mechanical behavior of single nanofiber and nanofiber layer of PCL/CNT composite nanofibers. This difference could be interesting in various applications such as tissue engineering [21].

For example, the mechanical properties of single nanofiber affect the stem cell differentiation, migration

F. Jahanmard-Hosseinabadi and M. Amani-Tehrani
Department of Textile Engineering, Amirkabir University of Technology, Tehran, Iran.

Correspondence should be addressed to M. Amani-Tehrani
e-mail: amani@aut.ac.ir

and proliferation, although the mechanical properties of nanofiber matrix are important for mechanical stability of tissues during tissue regeneration [22]. This example shows the significance of considering the mechanical properties of single nanofiber and nanofiber matrix, individually.

The mechanical properties of polymer/CNT composite nanofibers are completely dependent on CNT concentrations and dispersion quality [23]. In some cases, the higher CNT concentrations led to lower mechanical properties. The reason is that higher concentrations of CNTs lead to agglomeration of CNTs in nanofibers due to the high specific surface area of CNTs [24]. Meng *et al.* showed that 0.5 wt% concentration of CNT had better mechanical properties than 5 wt% [25]. However, most of the research only focuses on the mechanical properties of the nanofiber layers, not single nanofibers.

Although there are several reports on the examination of mechanical properties of PCL/CNT nanofibers, there is no report on a comparison between the mechanical properties of single nanofiber and nanofiber layer. Here, for the first time, the complete comparison was done between the mechanical properties of a single nanofiber and nanofiber layer by tensile testing.

II. EXPERIMENTAL

A. Materials and Methods

A.1. Preparation of PCL/F-MWCNTs Nanocomposite Nanofibers

A suspension of polycaprolactone (PCL) with functionalized-multiwall carbon nanotubes (F-MWCNTs) was prepared by dissolving 11 wt% poly(ε-caprolactone) (PCL, Mw 80,000; Sigma Aldrich) in chloroform (Merck). Then, the different amounts of COOH-multiwall carbon nanotubes (F-MWCNTs, >95%, OD 20-30 nm; US Research Nanomaterials) were dispersed in methanol (Merck) and sonicated by a probe sonicator (Hielscher Ultrasound Technology UIP1000hd) for 1 h to obtain a homogeneous and black dispersion. Then, the different concentrations of F-MWCNTs solutions were added dropwise to PCL solutions in a ratio of 1:3 with stirring. The final concentrations of F-MWCNTs were 0, 0.1, 0.5, 1, 2, and 3% with reference to PCL mass in the mixture. Before electrospinning, for each trial, the PCL/F-MWCNTs mixture was sonicated in an ultrasonic bath (Elma, Transsonic 460) for 1 h.

A conventional electrospinning process was used for fabrication of pure PCL nanofibers and PCL/F-MWCNTs nanocomposite nanofibers. Typically, the solutions were filled in a 1 mL plastic syringe and then electrospinning was performed at a flow rate of 1 mL/h. Indeed, the distance between the needle tip and the collector was adjusted to 17 cm and the solution was stretched under the high voltage of 18 kV. The nanofibers were electrospun in a constant temperature of 35 ºC and relative humidity of 35%. The random nanofibers were collected on a grounded rotary drum and the aligned nanofibers were collected between two parallel electrodes. Then the collected nanofibers were subsequently dried for at least 3 days under vacuum to remove any residual solvents.

A.2. Characterization

The morphology of the electrospun fiber coated with a thin layer of gold was observed by a scanning electron microscope (SEM) (Seron Technologies AIS2100, Korea). The average fiber diameter and fiber diameter distribution were calculated by measuring at least 50 nanofibers in one SEM image and five images were used for each layer using Image J. The porosity of nanocomposite nanofibers were calculated using Eq. (1):

$$P = 1 - \frac{\rho}{\rho'} \tag{1}$$

Where, P is the porosity of layer, ρ is the apparent density of layer and ρ′ the density of polymer materials used to fabricate the nanofibers. The apparent density was calculated with Eq. (2):

$$\frac{1}{\rho} = \frac{1}{\rho_{PCL}} + \frac{1}{\rho_{wt\%\ of\ CNTS}} \tag{2}$$

Where, ρ_{PCL} and ρ_{CNT} refer to the density of the PCL and F-MWCNTs, respectively.

The dispersion of F-MWCNTs in nanofibers was verified by transmission electron microscopy (TEM) (FEI Tecnai 12, Thermosystems-FEI, Eindhoven, the Netherlands) images. The nanofibers were prepared on grids with a Formvar-coated and carbon layer.

A.3. Mechanical Properties

A.3.1. Mechanical Properties of PCL/F-MWCNTs Nanocomposite Nanofibers

Mechanical properties of the nanocomposite nanofibers were obtained by testing rectangular samples with 5 mm wide and 20 mm length by using an Instron 5566 universal testing machine equipped with a 50 N load cell at a crosshead rate of 10 mm/min at ambient conditions.

A.3.2. Mechanical Properties of PCL/F-MWCNTs Single Nanofibers

Mechanical properties of the electrospun individual single

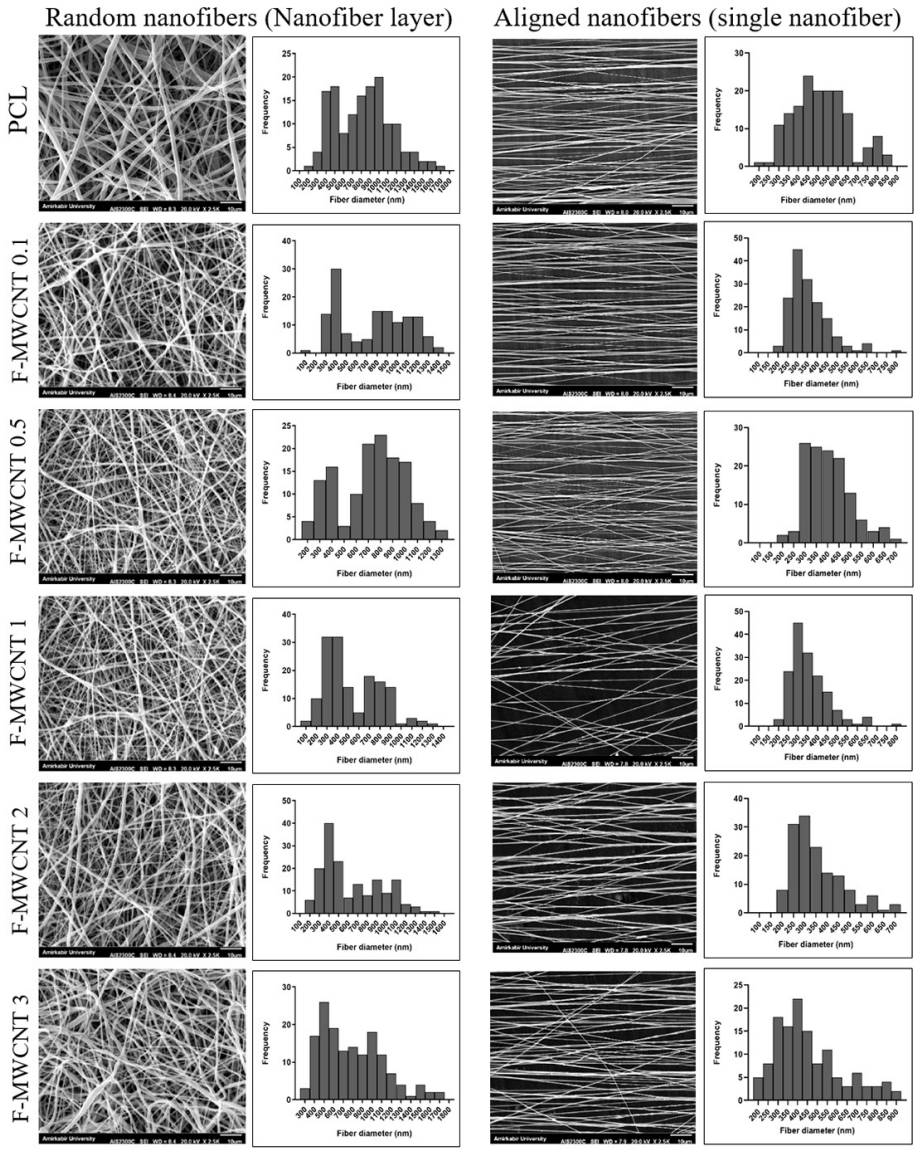

Fig. 1. Scanning electron microscope (SEM) images and distributions of fiber diameters of PCL electrospun nanofiber layers and aligned nanofibers with different concentrations of F-MWCNTs.

nanofibers were measured by using an Instron 5566 universal testing machine at a crosshead speed of 1 mm/min with a load cell of 50 N. All samples for the tensile test were prepared according to our previous report [26].

Briefly, since the mechanical properties of single nanofibers could be directly estimated from the mechanical properties of aligned nanofiber, two parallel electrodes were used for fabrication of aligned nanofibers. The nanofibers were separated by rectangular paper template from two electrodes, then the nanofibers with its template were mounted on the tensile tester machine. After this test, nanofibers were separated from the template and weighted by Pressley fiber-bundle strength tester.

A.4. Statistical Analysis

All quantitative datasets are expressed as mean ± SD. The One-Way ANOVA was performed to assess statistically significant differences in the results of different experimental groups. Values of ***$p<0.001$, **$p<0.01$, and *$p < 0.05$ were considered to be significantly different.

III. RESULTS AND DISCUSSION

A. Characterization

Fig. 1 shows the SEM micrographs and diameter distribution of PCL/F-MWCNTs composite nanofibers in different F-MWCNTs concentrations and different orientations (random and aligned). The uniform nanofibers were formed without an occurrence of the bead. The fiber

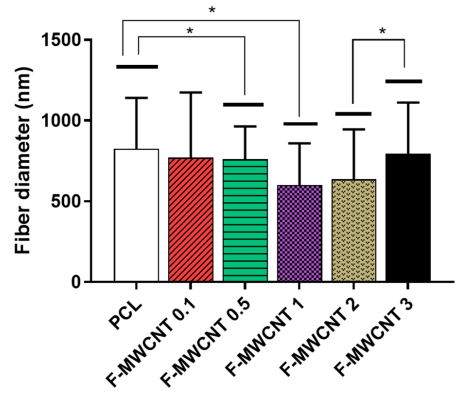

(a)

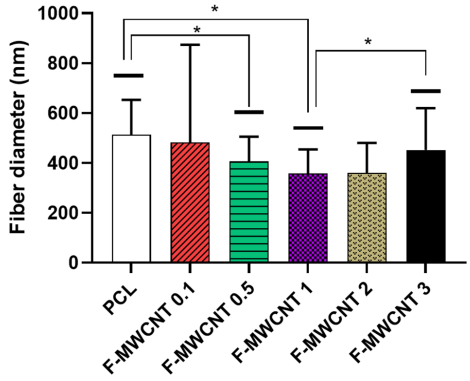

(b)

Fig. 2. Average fiber diameter of: (a) random nanofiber and (b) aligned nanofiber with various concentrations of F-MWCNTs (*P < 0.05).

distribution graph shows the high variation in nanofiber dimeters in both random and aligned layers.

The average fiber diameters of PCL nanofibers incorporated with 0.1 wt% to 1 wt% F-MWCNTs were smaller than those of PCL nanofibers without F-MWCNTs. However, further increase in F-MWCNTs content led to the increase of the average diameter of PCL/F-MWCNTs composite nanofibers (Fig. 2a). The reason is that the electrical conductivity of the solution increased as a result of the addition of the F-MWCNTs to the PCL solution. Therefore, the polymer solutions with a higher electrical conductivity resulted in thinner fibers [25]. On the other hand, the viscosity of the composite solutions increased upon adding F-MWCNTs into the PCL solution, which subsequently led to the formation of fiber with a thicker diameter [27]. Consequently, the formation of thinner nanofibers in this study resulted from enough solution flow and high electrical conductivity of the polymer solution due to the presence of 0.1 wt% to 1 wt% F-MWCNTs. Nevertheless, increasing the F-MWCNT concentration led to higher viscosity and subsequently thicker nanofiber diameter.

Fig. 2b shows that the average fiber diameters in aligned composite nanofiber layer are decreased with F-MWCNT concentration up to 1 wt% and then increased. In addition, the results show a similar trend for random nanofiber.

Fig. 3a reveals that F-MWCNTs are in alignment with the nanofiber axis at F-MWCNT concentration more than 1 wt%. This means that F-MWCNTs were completely dispersed in the polymer solution. Moreover, Fig. 3b shows that F-MWCNTs are agglomerated due to the high specific surface area of CNTs at F-MWCNT concentration more than 2 wt%.

B.1. Mechanical Properties of Individual Single PCL/F-MWCNTs Fiber

To measure the mechanical properties of single nanofiber, the samples were prepared as shown in Fig. 4 according to previous work by the authors [26]. Briefly, the mechanical properties of single nanofibers could be directly estimated from the mechanical properties of the completely aligned

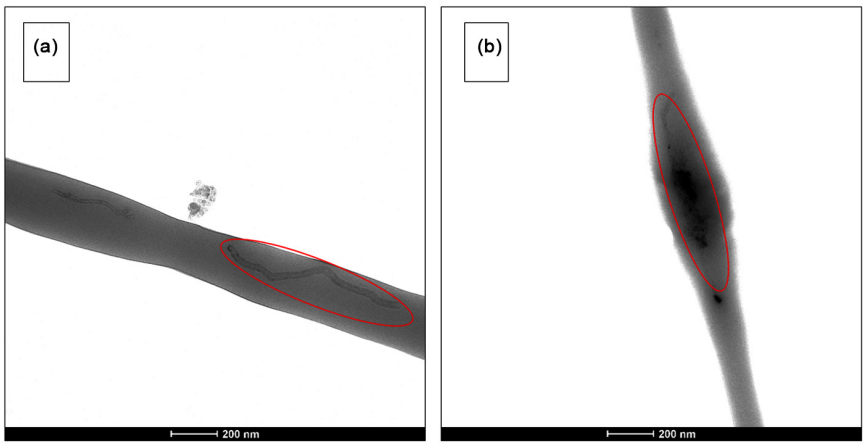

Fig. 3. TEM images of composite nanofibers containing: (a) 1 wt% F-MWCNTs and (b) 2 wt% F-MWCNTs.

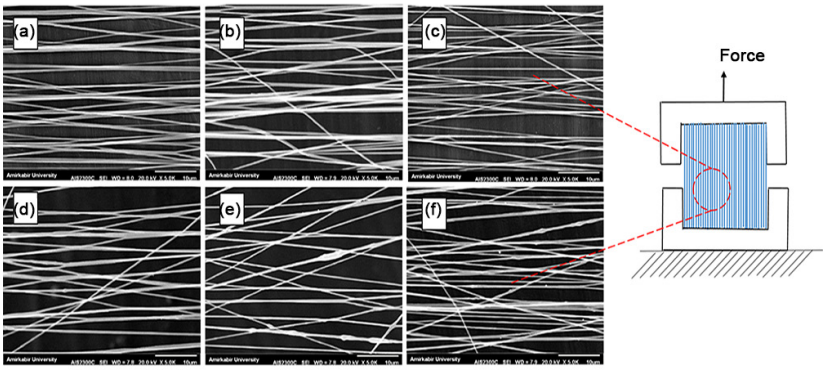

Fig. 4. SEM images of aligned PCL/F-MWCNT nanofibers with: (a) 0, (b) 0.1, (c) 0.5, (c) 1, (e) 2, and (f) 3 wt% F-MWCNT concentration, and (g) tensile test set-up for prepared aligned nanofiber samples.

nanofiber that was preferentially produced by two parallel electrodes with a defined fiber orientation index.

The surface area of the neatly aligned nanofiber layer (where the voids between the nanofibers were neglected) was determined by the density-based method (Eq. (3)):

$$A = \frac{W}{L_{0\rho}} \tag{3}$$

Where, W and L_0 represent the weight and length of the nanofiber sample, respectively, and ρ is the density of composite material (PCL/MWCNTs). The ρ was calculated with Eq. (2). In the following, the young modulus of the nanofiber layer is obtained by Eq. (4):

$$E_T = \frac{F/A}{\Delta L / L_0} \tag{4}$$

Where, F is the force exerted on the nanofibers under tension, A is the cross-sectional area of nanofiber through which the force is applied, ΔL defines the length change of nanofibers, and L_0 is the original length of the nanofibers.

According to a previous report by the authors [26], Young's modulus of single nanofibers could be directly estimated from the modulus of an aligned nanofiber. Whereas the probability density function of all electrospun aligned nanofibers in this experiment is a Cauchy distribution, Young's modulus of a single nanofiber can be calculated by Eq. (5):

$$\frac{E_T}{E_S} = \frac{1}{\gamma\pi}\int_{-\frac{\pi}{2}}^{\frac{\pi}{2}} \frac{1}{(1+((\theta/\gamma)^2)}\cos\theta \, d\theta \tag{5}$$

Where, E_T is Young's modulus of an aligned nanofiber, E_S is Young's modulus of single nanofiber, γ and θ refer to the scale factor of the Cauchy distribution and the orientation angle of the nanofibers in the layer, respectively.

Fig. 5 shows the relationship between the scale parameter and orientation index of aligned nanofibers at different F-MWCNT concentrations for measuring the single nanofiber modulus.

Fig. 6 shows that the relation between the standard deviation of the Cauchy distribution and orientation index is linear and Eq. (6) is obtained from the best-fitted line to orientation index of the aligned nanofiber.

The orientation index could be obtained directly from the orientation j plugin in order to determine the scale factor.

$$\gamma = -0.1574\ O_i + 15.626 \tag{6}$$

Where, γ is the scale factor of fitted Cauchy distribution and O_i is the orientation index of nanofibers.

As shown in Table I, Young's modulus of single nanofibers increases with increasing F-MWCNTs up to 1 wt%. Thus, PCL with 0.5 wt% to 1 wt% F-MWCNTs exhibited the maximum modulus. The good dispersion of F-MWCNTs in the polymer layer provided a more uniform stress distribution and minimized the presence of stress-concentration centers. The good dispersion also increased the interfacial area needed for stress transfer from the polymer layer to the F-MWCNTs [25]. Subsequently, further increasing the filler content (2 and 3 wt%) led to a decrease in the PCL/F-MWCNT nanofiber modulus because the nanomaterials have high surface energy and are more susceptible to aggregation [28].

C. Comparison Between Mechanical Properties of Nanofiber Layer and Single Nanofibers

In addition to the single nanofiber mechanical properties, the interaction between nanofibers in the fibrous layer can also contribute to the mechanical properties of the

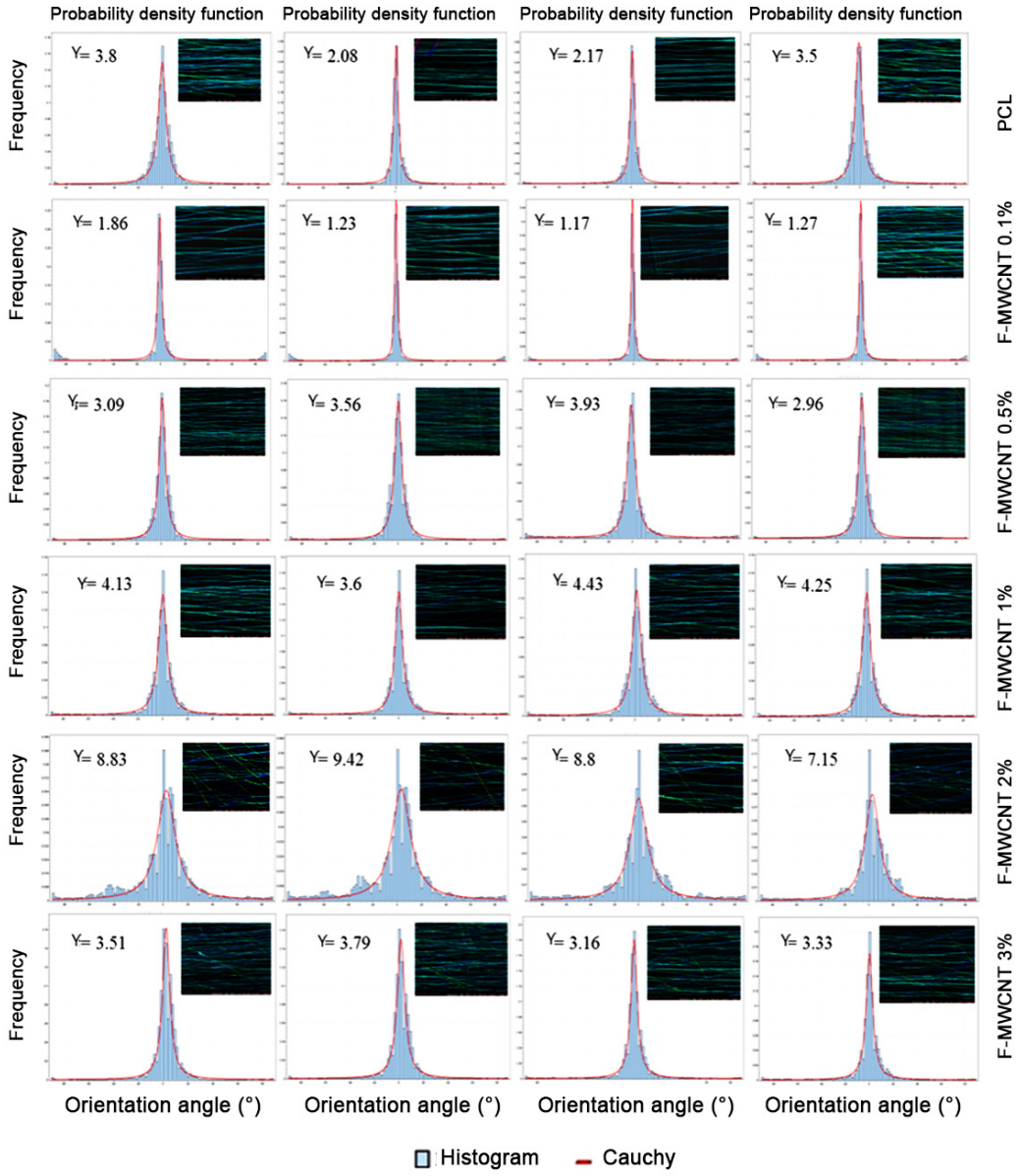

Fig. 5. Orientation angle histograms of aligned nanofiber with different F-MWCNT concentrations and fitted Cauchy distribution.

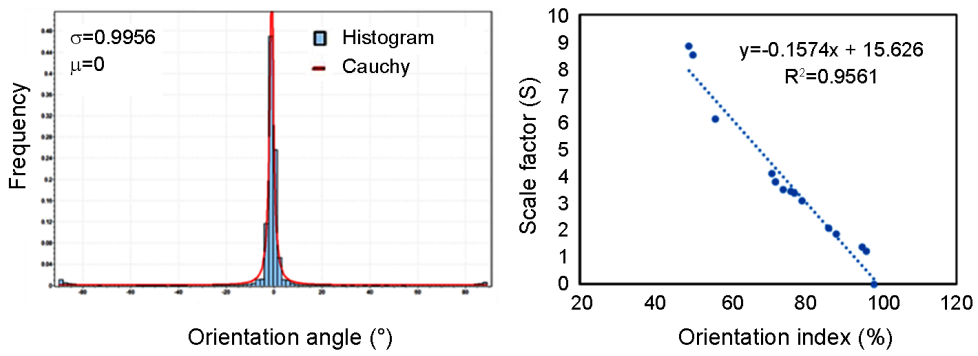

(a) (b)

Fig. 6. (a) Probability density function of aligned nanofiber and (b) linear correlation between orientation index and the standard deviation of the fitted density function.

TABLE I
YOUNG'S MODULUS OF INDIVIDUAL SINGLE PCL NANOFIBER AS A FUNCTION OF F-MWCNT CONTENT

	Orientation index (%)	Scale parameter (%)	E_T (MPa)	E_s (MPa)
PCL	80.93±5.1	2.89±0.77	344.02±27.28	362.13±27.28
F-MWCNT 0.1	90.49±6.9	1.38±0.28	415.89±42.57	424.37±42.57
F-MWCNT 0.5	77.77±7.5	3.38±0.38	434.94±46.37	457.83±46.37
F-MWCNT 1	73.21±7.5	4.10±0.31	444.91±43.11	473.3±43.11
F-MWCNT 2	64.01±5.1	5.55±0.85	353.57±43.33	371.57±43.33
F-MWCNT 3	77.37±5.2	3.45±0.23	277.61±35.80	292.22±35.80

layer [29].

The stress-strain curves shown in Fig. 7 were used to characterize the mechanical performance of the nanofiber layer and single nanofiber.

Table II shows methods used for nanofiber preparation as well as measuring and calculating the mechanical properties of the nanofiber layer and single nanofiber.

Figs. 8a and 8b show Young's modulus and tensile strength trends for single nanofibers and nanofiber layer. The Young's modulus and tensile strength of the nanofiber layer increased when the F-MWCNT concentration was increased. However, Young's modulus and tensile strength of a single nanofiber increased with increasing F-MWCNTs up to 1 wt% and then decreased. In addition, Figs. 8a and 8b show higher tensile strength and modulus for single nanofibers compared to those for nanofiber layer. This is likely due to the random orientation of the nanofiber layer. Therefore, in this case, more than single nanofiber modulus, the cohesion between nanofibers at nanoscale contact point could change the mechanical behavior of the nanofiber layer [29].

Figs. 8c and 8d reveal that the toughness and strain for the nanofiber layer were higher than those for single nanofibers. Moreover, the toughness and strain for the nanofiber layer increased with increasing F-MWCNTs up to 2 wt% and then decreased. The single nanofiber toughness increased with with increasing F-MWCNTs up to 1 wt% and then decreased. However, the strain of single nanofiber increased when the F-MWCNT concentration was increased. The strain and toughness of the nanofiber layer were higher than those of single nanofiber. The reason

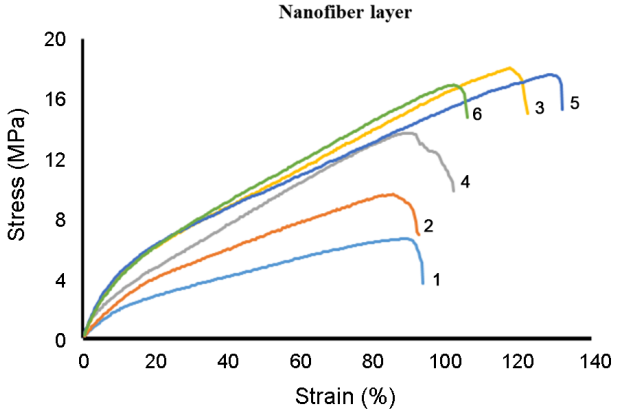

(a)

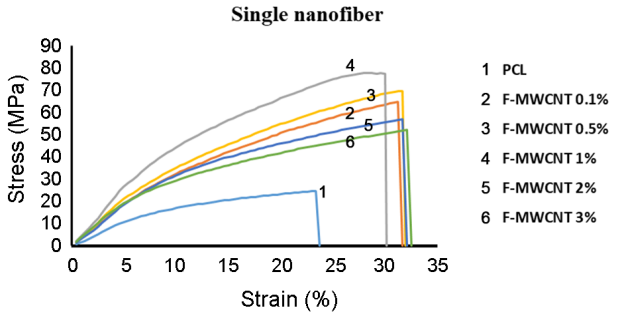

(b)

Fig. 7. Representative tensile stress-strain curves for the electrospun PCL/F-MWCNT composite nanofibers and individual single nanofiber with various F-MWCNT concentrations.

TABLE II
METHODS FOR PREPARATION AND MECHANICAL ANALYSIS OF NANOFIBER LAYER AND SINGLE NANOFIBER

	Nanofiber layer (random nanofiber)	Single nanofiber
Preparation methods	Rotary drum (rpm:400)	Two parallel electrodes (aligned nanofiber)
Mechanical tests	Tensile tester (Instron)	Tensile tester (Instron)
Methods for calculating the mechanical properties	Density-based method (DBM)	Density-based method (DBM) for obtaining E_T and Eq. (5) for calculating E_s

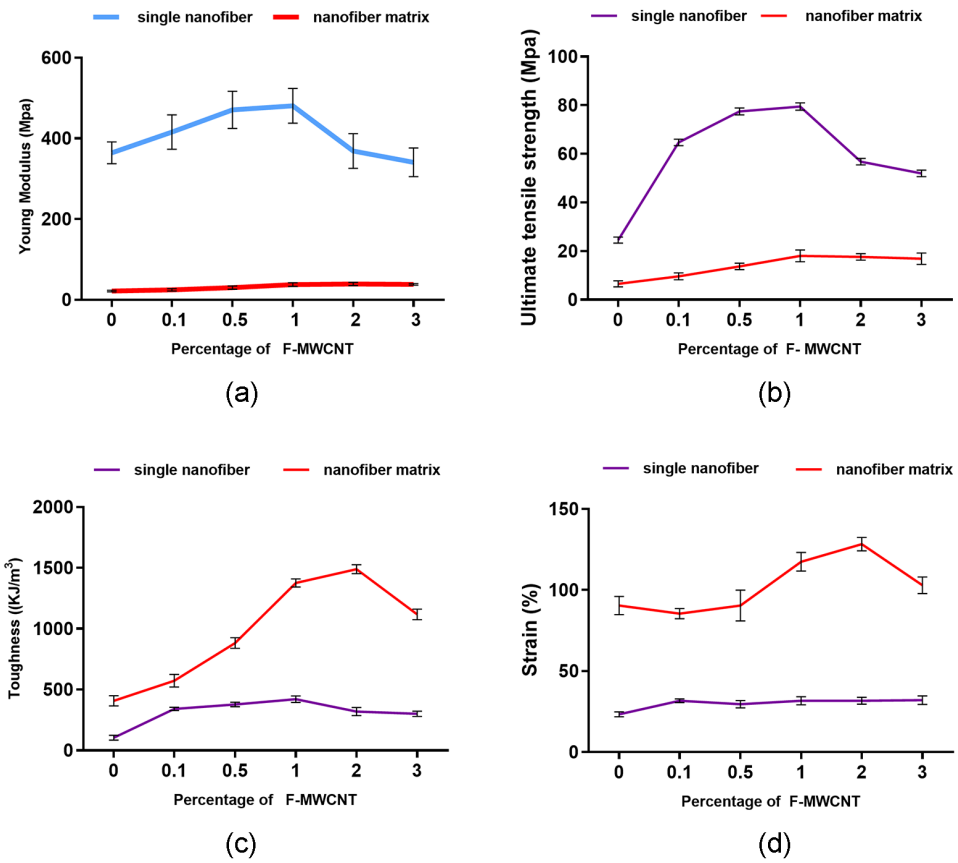

Fig. 8. Mechanical properties of PCL/F-MWCNT composite nanofibers: (a) Young's modulus, (b) ultimate tensile strength, (c) toughness, and (d) strain for composite nanofiber layer and individual single nanofibers with various F-MWCNT concentrations.

is that existing fibers in nanofiber layer due to random orientation tried to reorient themselves in the applied force direction and subsequently they elongated more than single nanofibers.

Comparison between the mechanical properties of the PCL/F-MWCNT nanofiber layer and single nanofiber showed that the addition of F-MWCNTs into the PCL influenced the mechanical properties of the composite nanofibers. As a nanofiller, F-MWCNTs with a lower concentration (0.1–1 wt% F-MWCNTs) could disperse in the PCL polymer matrix very well and transferred the stress from the layer to the CNT. This led to better mechanical properties for single nanofiber. This reinforcement could be associated with the excellent intrinsic properties of the carbon nanotube, the uniform dispersion of the F-MWCNTs in the PCL layer and the interactions between the F-MWCNT nanofillers and polymer layer [25,28]. By adding more than 1 wt% of F-MWCNTs, the nanofillers became agglomerate and the mechanical properties of single nanofiber decreased. Nevertheless, the mechanical properties of the layer improved once the F-MWCNT concentration increased. The different trend in the mechanical properties of single nanofiber and nanofiber layer with increasing F-MWCNT concentration may be due to the randomness structure of nanofibers in the layer, cohesion among nanofibers at contact points and variation in the nanofiber diameters [25].

IV. CONCLUSION

In this study, PCL/F-MWCNT composite nanofibers with various percentage of F-MWCNTs were fabricated by electrospinning. A comprehensive comparison was done between the mechanical properties of the nanofiber layer and single nanofibers of composite structures. The comparison between composite nanofibers with various concentration of F-MWCNT demonstrated that the mechanical properties of the nanofiber layer and single nanofibers had significant differences. Because more than mechanical properties of single nanofibers, other factors such as fiber diameters, randomness structure, and interaction between nanofibers can affect the mechanical

properties of the layer. In conclusion, tailoring mechanical properties of both single nanofibers and nanofiber layeris the main step towards designing the desired substrate for a different application.

REFERENCES

[1] K.P. Feltz, E.A.G. Kalaf, C. Chen, R.S. Martin, and S.A. Sell, "A review of electrospinning manipulation techniques to direct fiber deposition and maximize pore size", *Electrospinning*, vol. 1, no. 1, pp. 46-61, 2017.

[2] H. Kriel, M. Coates, and A. Smit, "Electrospun Fibers for Advanced Wound Care: Moving from Novel Lab-Scale Curiosities to Commercial Realities", in *Electrospinning: From Basic Research to Commercialization*, 2018, pp. 95-135.

[3] J. Hu, D. Kai, H. Ye, L. Tian, X. Ding, S. Ramakrishna, and X.J. Loh, "Electrospinning of poly(glycerol sebacate)-based nanofibers for nerve tissue engineering", *Mat. Sci. Eng. C*, vol. 70, pp. 1089-1094, 2017.

[4] M.R. Casanova, R.L. Reis, A. Martins, and N.M. Neves, "Nanotechnology, Scaffolding-Related Developments and Translation", in *The Use of Electrospinning Technique on Osteochondral Tissue Engineering, Osteochondral Tissue Engineering*, 2018, pp. 247-263.

[5] V. Mouriño, "Nanoelectrospun Matrices for Localized Drug Delivery", in *Applications of Nanocomposite Materials in Drug Delivery*, Elsevier, 2018, pp. 491-508.

[6] A. Khalf and S.V. Madihally, "Recent advances in multiaxial electrospinning for drug delivery", *Eur. J. Pharm. Biopharm.*, vol. 112, pp. 1-17, 2017.

[7] R. Halaui, E. Zussman, R. Khalfin, R. Semiat, and Y. Cohen, "Polymeric microtubes for water filtration by co-axial electrospinning technique", *Polym. Adv. Technol.*, vol. 28, no. 5, pp. 570-582, 2017.

[8] H. Gao, Y. Yang, O. Akampumuza, J. Hou, H. Zhang, and X. Qin, "A low filtration resistance three-dimensional composite membrane fabricated via free surface electrospinning for effective PM 2.5 capture", *Env. Sci. Nano*, vol. 4, no. 4, pp. 864-875, 2017.

[9] M. Zhang, X. Zhao, G. Zhang, G. Wei, and Z. Su, "Electrospinning design of functional nanostructures for biosensor applications", *J. Mater. Chem. B*, vol. 5, no. 9, pp. 1699-1711, 2017.

[10] P. Ekabutr, W. Klinkajon, P. Sangsanoh, O. Chailapakul, P. Niamlang, T. Khampieng, and P. Supaphol, "Electrospinning: a carbonized gold/graphene/PAN nanofiber for high performance biosensing", *Anal. Methods-UK*, vol. 10, no. 8, pp. 874-883, 2018.

[11] S. Chawla, J. Cai, and M. Naraghi, "Mechanical tests on individual carbon nanofibers reveals the strong effect of graphitic alignment achieved via precursor hot-drawing", *Carbon*, vol. 117, pp. 208-219, 2017.

[12] A. Morel, S. Domaschke, V.U. Kumaran, D. Alexeev, A. Sadeghpour, S.N. Ramakrishna, S.J. Ferguson et al., "Correlating diameter, mechanical and structural properties of poly(L-lactide) fibres from needleless electrospinning", *Acta Biomater.*, vol. 81, pp. 169-183, 2018.

[13] K. Sakakibara, Y. Moriki, H. Yano, and Y. Tsujii, "Strategy for the improvement of the mechanical properties of cellulose nanofiber-reinforced high-density polyethylene nanocomposites using diblock copolymer dispersants", *ACS Appl. Mater. Inter.*, vol. 9, no. 50, pp. 44079-44087, 2017.

[14] S.G. King, N.J. Terrill, A.J. Goodwin, R. Stevens, V. Stolojan, and S.R.P. Silva, "Probing of polymer to carbon nanotube surface interactions within highly aligned electrospun nanofibers for advanced composites", *Carbon*, vol. 138, pp. 207-214, 2018.

[15] X.-L. Xie, Y.-W. Mai, and X.-P. Zhou, "Dispersion and alignment of carbon nanotubes in polymer matrix: a review", *Mater. Sci. Eng. R Rep.*, vol. 49, no. 4, pp. 89-112, 2005.

[16] G. Mittal, V. Dhand, K.Y. Rhee, S.-J. Park, and W.R. Lee, "A review on carbon nanotubes and graphene as fillers in reinforced polymer nanocomposites", *J. Ind. Eng. Chem.*, vol. 21, pp. 11-25, 2015.

[17] V.D. Punetha, S. Rana, H.J. Yoo, A. Chaurasia, J.T. McLeskey Jr, M.S. Ramasamy, N.G. Sahoo et al., "Functionalization of carbon nanomaterials for advanced polymer nanocomposites: a comparison study between CNT and graphene", *Prog. Polym. Sci*., vol. 67, pp. 1-47, 2017.

[18] R. Rafiee and R. Pourazizi, "Influence of CNT functionalization on the interphase region between CNT and polymer", *Comp. Mater. Sci.*, vol. 96, pp. 573-578, 2015.

[19] L.A. Mercante, A. Pavinatto, L.E. Iwaki, V.P. Scagion, V. Zucolotto, O.N. Oliveira Jr, L.H. Mattoso et al., "Electrospun polyamide 6/poly(allylamine hydrochloride) nanofibers functionalized with carbon nanotubes for electrochemical detection of dopamine", *ACS Appl. Mater. Inter.*, vol. 7, no. 8, pp. 4784-4790, 2015.

[20] G. Abagnale, A. Sechi, M. Steger, Q. Zhou, C.-C. Kuo, G. Aydin, C. Schalla et al., "Surface topography guides morphology and spatial patterning of induced pluripotent stem cell colonies", *Stem Cell Rep.,* vol. 9,

no. 2, pp. 654-666, 2017.

[21] F.J.H. Abadi, M.A. Tehran, F. Zamani, M. Nematollahi, L.G. Mobarakeh, and M.H. Nasr-Esfahani, "Effect of nanoporous fibers on growth and proliferation of cells on electrospun poly(ϵ-caprolactone) scaffolds", *Int. J. Polym. Mater. Po.*, vol. 63, no. 2, pp. 57-64, 2014.

[22] K.M. Kennedy, A. Bhaw-Luximon, and D. Jhurry, "Cell-matrix mechanical interaction in electrospun polymeric scaffolds for tissue engineering: implications for scaffold design and performance", *Acta Biomater.,* vol. 50, pp. 41-55, 2017.

[23] G.-Y. Liao, X.-P. Zhou, L. Chen, X.-Y. Zeng, X.-L. Xie, and Y.-W. Mai, "Electrospun aligned PLLA/PCL/functionalised multiwalled carbon nanotube composite fibrous membranes and their bio/mechanical properties", *Compos. Sci. Technol.*, vol. 72, no. 2, pp. 248-255, 2012.

[24] K. Saeed, S.-Y. Park, H.-J. Lee, J.-B. Baek, and W.-S. Huh, "Preparation of electrospun nanofibers of carbon nanotube/polycaprolactone nanocomposite", *Polymer*, vol. 47, no. 23, pp. 8019-8025, 2006.

[25] Z.X. Meng, W. Zheng, L. Li, and Y.F. Zheng, "Fabrication and characterization of three-dimensional nanofiber membrance of PCL–MWCNTs by electrospinning", *Mater. Sci. Eng. C*, vol. 30, no. 7, pp. 1014-1021, 2010.

[26] F. Jahanmard-Hosseinabadi, M. Amani-Tehran, and M.B. Eslaminejad, "Mathematical modeling and experimental evaluation for the predication of single nanofiber modulus", *J. Mech. Behav. Biomed.*, vol. 79, pp. 38-45, 2018.

[27] M. Shtein, I. Pri-Bar, and O. Regev, "A simple solution for the determination of pristine carbon nanotube concentration", *Analyst*, vol. 138, no. 5, pp. 1490-1496, 2013.

[28] Y. Liu and S. Kumar, "Polymer/carbon nanotube nano composite fibers–a review", *ACS Appl. Mater. Inter.,* vol. 6, no. 9, pp. 6069-6087, 2014.

[29] Q. Shi, S.-C. Wong, W. Ye, J. Hou, J. Zhao, and J. Yin, "Mechanism of adhesion between polymer fibers at nanoscale contacts", *Langmuir*, vol. 28, no. 10, pp. 4663-4671, 2012.